(16) Muthukumar, M. *J. Chem. Phys.* **1985**, *83*, 3161.
(17) Vilgis, T. A. *Phys. Rev. A* **1987**, *36*(3), 1506.
(18) Eichinger, B. E.; Martin, J. *Macromolecules* **1980**, *13*, 626.
(19) de Gennes, P. G. *Scaling Concepts in Polymer Science*; Cornell University Press: Ithaca, NY, 1979.
(20) Doi, M.; Edwards, S. F. *J. Chem. Soc., Faraday Trans. 2* **1978**, *74*, 1789.
(21) Fölsch, K. J. Dissertation, Mainz, 1988.

# Order–Disorder Transition of Star Block Copolymers. 2. Effect of Arm Number

**Yasuhito Ijichi and Takeji Hashimoto***

*Department of Polymer Chemistry, Kyoto University, Kyoto 606, Japan*

**Lewis J. Fetters**

*Corporate Research Laboratories, Exxon Research and Engineering Company, Clinton Township, Annandale, New Jersey 08801.* *Received August 23, 1988; Revised Manuscript Received November 21, 1988*

ABSTRACT: Ordered structure, order–disorder transition, and the thermal concentration fluctuations in the disordered state were investigated by the small-angle X-ray scattering (SAXS) method, for a series of poly(styrene–isoprene) star block copolymers having a fixed molecular weight and composition for the arm diblock copolymer but a different number of arms ($n$ = 1–18). The characteristic length $D_{ord}(n,T)$ of the order parameter $\psi(\mathbf{r};T)$ in the ordered state was found to obey $D_{ord}(n,T) = D_{dis}(n)(T/T_b)^{-1/3}$ where $D_{dis}$ is the characteristic length of $\psi(\mathbf{r};T)$ in the disordered state, which was found to obey $D_{dis}(n,T) = f(n)T^0$, $f(n)$ being a weak function of $n$ as seen in $q_{max}(n)$ in the paper. The order–disorder temperature $T_b$ and spinodal temperature $T_s$ were found to be almost independent of $n$ for $n > 2$. The SAXS profiles from the disordered state were found to be fitted quite well with the theoretical profiles given by a mean-field random-phase approximation. The analyses yielded a remarkable $n$-dependence of the Flory–Huggins interaction parameter $\chi$, $\chi$ decreasing with increasing $n$. The analyses yielded also the values $D_{dis}$ (defined as $D_{dis,exp}$) and $\chi$ at the spinodal point (defined as $\chi_{s,exp}$). These values were compared with the corresponding theoretical values $D_{dis,theor}$ and $\chi_{s,theor}$; $\chi_{s,theor} \simeq \chi_{s,exp}$ and $D_{dis,exp} \simeq 1.1\ D_{dis,theor}$, irrespective of the value $n$.

## I. Introduction

Experimental and theoretical investigations of the thermal concentration fluctuations of the constituent components for the two-component polymer systems, polymer A and polymer B, are one of the important subjects in condensed-state polymer physics.[1-18] The main interests involve the exploration of the effects of chemical connectivity on the fluctuation spectra or, in more general sense, on the physics of cooperative phenomena.

Here in this paper we deal with two kinds of *connectivity*, (i) the connectivity of monomers A and B in polymers A and B (the "first-kind connectivity") and (ii) the connectivity of different polymers A and B (the "second-kind connectivity"), giving rise to A–B type linear block polymers,[2-4,7-9] grafted polymers,[6,8] and star block copolymers.[6,8] It has been found that the latter connectivity generates the dominant mode of the concentration fluctuations with a wavenumber $q = q_{max}$ other than zero in both the ordered and disordered state. The connectivity induces the thermodynamic instability[3] also at $q \neq 0$. The growth of the dominant mode of the fluctuations with $q_{max} \neq 0$ is known traditionally as "microphase separation" or recently "microphase-separation transition"[3] or "order–disorder transition",[11] in contrast to the ordinary liquid–liquid phase transition for the mixtures of polymers A and B, which causes the growth of the fluctuations with $q_{max} = 0$. Thus, this kind of the order–disorder transition is a unique cooperative phenomenon inherent to polymer systems.

In this paper we further focus our interests on the effects of the second-kind connectivity on the spectra of the spatial concentration fluctuations of A and B monomers at thermal equilibrium by selecting a series of star block copolymers as a model system. The starblock copolymers were prepared by chemically connecting a poly(styrene–isoprene) diblock polymer with a given total polymerization index and a given fraction of styrene and isoprene where the polystyrene block was the outer segments. We studied a series of copolymers having different arm numbers $n$ by small-angle X-ray scattering (SAXS) and analyzed the order parameter $\psi$ (the concentration fluctuations of the constituent monomeric units) both in the ordered and disordered states as well as the order–disorder transition as a function of $n$. The fluctuation spectra in the disordered state will be compared with those predicted by a current theory of a mean-field random-phase approximation, first presented by de la Cruz and Sanchez[6] and later by others.[8,18]

Our analyses are restricted to the mean-field approach. A more general analysis including nonclassical effects (Brazovskii effect) as suggested first by Leibler[3] and calculated by Fredrickson and Helfand[19] for diblock copolymers will be very important. However, that kind of a generalized analysis is beyond the scope of this paper. This work is an extension of earlier work by Fetters, Richards, and Thomas[20] on the composition dependence of the fluctuations of the star block copolymers in the disordered state and by Hashimoto, Ijichi, and Fetters[18] on star block copolymers with $n$ = 1 and 6.

This paper is constructed as follows. We first describe experimental methods (section II), theoretical background (section III), and some selected typical experimental results (section IV). We then present some theoretical interpretations on the fluctuations in the ordered state (section V-A), the fluctuation spectra in the disordered state (section V-B), the estimated Flory–Huggins thermody-

0024-9297/89/2222-2817$01.50/0 

**Table I**
**Block Copolymer Characterization**

| | PS block | | diblock copolymers | | | star block copolymer | | |
|---|---|---|---|---|---|---|---|---|
| sample | $M_n \times 10^{-4}$ [a] | $M_w/M_n$ [a] | $M_n \times 10^{-4}$ [b] | $M_w/M_n$ [a] | wt % [c] PS | $M_n \times 10^{-5}$ [b] | $M_w/M_n$ [a] | $n$ [d] |
| SI-1/30/10 | 1.00 | 1.02 | 3.30 | 1.03 | 30.3 | | | 1 |
| SI-2/30/10 [e] | 1.00 | 1.02 | 3.30 | 1.03 | 30.3 | 0.67 | 1.03 | 2.0 |
| SI-3/30/10 | 1.00 | 1.02 | 3.32 | 1.03 | 30.2 | 0.99 | 1.03 | 3.0 |
| SI-4/30/10 [f] | 1.00 | 1.03 | 3.40 | 1.05 | 29.5 | 1.32 | 1.04 | 3.9 |
| SI-5/31/10 [g] | 1.04 | 1.05 | 3.36 | 1.04 | 30.9 | 1.65 | 1.03 | 4.9 |
| SI-6/31/10 [g] | 1.04 | 1.05 | 3.36 | 1.04 | 30.9 | 2.00 | 1.03 | 6.0 |
| SI-8/30/10 [f] | 1.00 | 1.03 | 3.40 | 1.05 | 29.5 | 2.64 [h] | 1.04 | 7.8 |
| SI-12/30/10 [f] | 1.00 | 1.03 | 3.40 | 1.05 | 29.5 | 4.10 [h] | 1.04 | 12.1 |
| SI-18/35/10 | 1.00 | 1.02 | 2.80 | 1.04 | 35.0 | 4.93 [h] | 1.05 | 17.6 |

[a] Via size exclusion chromatography. [b] Via membrane osmometry. [c] Via $^1$H NMR. [d] Number of arms; $n = M_n(\text{star})/M_n(\text{arm})$ or $M_w(\text{star})/M_n(\text{arm})$. [e] This linear triblock was made via coupling SI-1/30/10 with $Cl_2Si(CH_3)_2$. [f] This series was made using the same diblock arm. [g] These two-star copolymers were made using the same diblock arm. [h] $M_w$ via light scattering in THF.

namic interaction parameter (section V-C), the stability limits (section V-D), and the wavenumber of $q_{max}$ for the dominant mode of the fluctuations in the disordered state (section V-E), as a function of $n$.

## II. Experimental Methods

The sample preparations, measurements of SAXS, and their data treatment and corrections were described in the companion paper[18] and will not be repeated here. We described here the most important features and the features added in this paper.

The linear poly(styrene-*block*-isoprene) diblock copolymer (corresponding the starblock with the arm number $n = 1$) and $n$-arm poly(styrene-*block*-isoprene) starblock copolymers were prepared by anionic polymerization. The star block copolymers were synthesized by chemically connecting the diblock copolymers at the ends of each polyisoprene block, and the polystyrene block was the outer segment. The polystyrene segments and the poly(styrene-*block*-isoprene) diblock polymers (SI) had nearly monodisperse molecular weight distributions. The molecular parameters for the star block copolymers used in this study are given in Table I. The nomenclature used to describe these materials is that used previously,[21] e.g., SI-$n$/31/10 where the first digit denotes the number of arms, the second the weight percent of polystyrene, and the third the molecular weight of the polystyrene segment in kg mol$^{-1}$.

The copolymers were found to have high order–disorder transition temperatures $T_b$ in bulk ($T_b \gtrsim 180$ °C), which makes quantitative SAXS analyses difficult over a reasonably wide range of temperatures in the disordered state because of thermal instability of the copolymers at high temperatures $T > T_b$. In order to circumvent this difficulty we added a small amount of a neutral solvent, dioctyl phthalate (DOP), to the copolymers. The volume fraction of polymer ($\phi_p$) in the solutions studied here is 0.6 for the copolymer with $n = 1$ or 0.8 for the copolymers with $n \geq 2$.

## III. Theoretical Background

In the ordered state, polystyrene (PS) block chains and polyisoprene (PI) block chains segregate themselves into the respective domains to form microdomains in an ordered lattice.[11] We analyzed the Bragg spacing $D$ as a parameter associated with the characteristic size of the order parameter fluctuation in the ordered state from the magnitude of the scattering vector $q_{max}$ at which the first-order scattering maximum locates

$$D = 2\pi q_{max}^{-1} \tag{1}$$

where $q_{max}$ is $q$ at the scattering angle $2\theta = 2\theta_m$ of the first-order peak

$$q = (4\pi/\lambda) \sin \theta \tag{2}$$

$\lambda$ (=1.54 Å) and $2\theta$ are the wavelength and the scattering angle, respectively. The scattering intensity $I(q)$ for the starblock copolymers in the bulk disordered state was first presented by de la Cruz and Sanchez by using the path integral method (eq 28 of ref 6). The identical equation was obtained also by other methods.[8,18] In the context of the mean-field random-phase approximation (RPA), $I(q)$ for the two-component polymer systems is generally given by[3]

$$I(q) = (a - b)^2[S(q)/W(q) - 2\chi]^{-1} \tag{3}$$

$$S(q) = S_{AA}(q) + S_{BB}(q) + 2S_{AB}(q) \tag{4}$$

$$W(q) = S_{AA}(q)S_{BB}(q) - S_{AB}(q)^2 \tag{5}$$

where $a - b$ is the difference of the scattering contrast (electron density for SAXS) between the components A and B, and $S_{ij}(q)$ ($i,j$ = A or B) is the $q$ Fourier component of the density–density correlation functions between $i$ and $j$ monomers for Gaussian chains.

The function $S_{ij}(q)$'s for the particular type of star block copolymers that we are dealing with here are given by[18]

$$S_{ij}(q) = nS_{ij}^{\alpha}(q) + n(n - 1)S_{ij}^{\beta}(q) \tag{6}$$

where $n$ is the number of arms. $S_{ij}^{\alpha}(q)$ and $S_{ij}^{\beta}(q)$ stand for, respectively, $S_{ij}(q)$'s for the two monomers in the same arm and in different arms

$$S_{AA}^{\alpha}(q) = (nN_0)^{-1}g_2(f,N_0) \tag{7}$$

$$S_{AA}^{\beta}(q) = (nN_0)^{-1}(1/2)\{g_2(f,2N_0) - 2g_2(f/2,2N_0)\} \tag{8}$$

$$S_{BB}^{\alpha}(q) = (nN_0)^{-1}g_2(1-f,N_0) \tag{9}$$

$$S_{BB}^{\beta}(q) = (nN_0)^{-1}(1/2)\{g_2(1,2N_0) - 2g_2[(1+f)/2,2N_0] + g_2(f,2N_0)\} \tag{10}$$

$$S_{AB}^{\alpha}(q) = (nN_0)^{-1}(1/2)\{g_2(1,N_0) - g_2(1-f,N_0) - g_2(f,N_0)\} \tag{11}$$

$$S_{AB}^{\beta}(q) = (nN_0)^{-1}(1/2)\{g_2[(1+f)/2,2N_0] - g_2(1/2,2N_0) - g_2(f,2N_0) + g_2(f/2,2N_0)\} \tag{12}$$

$$g_2(f,N_0) = (2/y^2)\{fN_0y + \exp(-fN_0y) - 1\} \tag{13}$$

$$y = q^2a^2/6 \tag{14}$$

where $N_0$ is the polymerization index of each arm, $f$ is defined as $N_A/N_0$, and $a$ is the Kuhn statistical segment length of A and B block sequences. Here, A and B are assumed to have identical segment length, and $N_A$ is the polymerization index of the A block sequence whose end is connected to the core of the star. The details of the calculation processes can be found in our previous paper.[18]

The equation for the bulk was applied to the solutions with $\phi_p = 0.6$ or 0.8 just by replacing $\chi$ and $(a - b)^2$ in eq 3 by corresponding *effective values* $\chi_{eff}$ and $(a - b)_{eff}^2$ (pseudobinary approximation).[22,23]

## IV. Experimental Results

Figure 1 shows typical desmeared SAXS profiles[24] for the star block copolymer with $n = 3$ at temperatures from

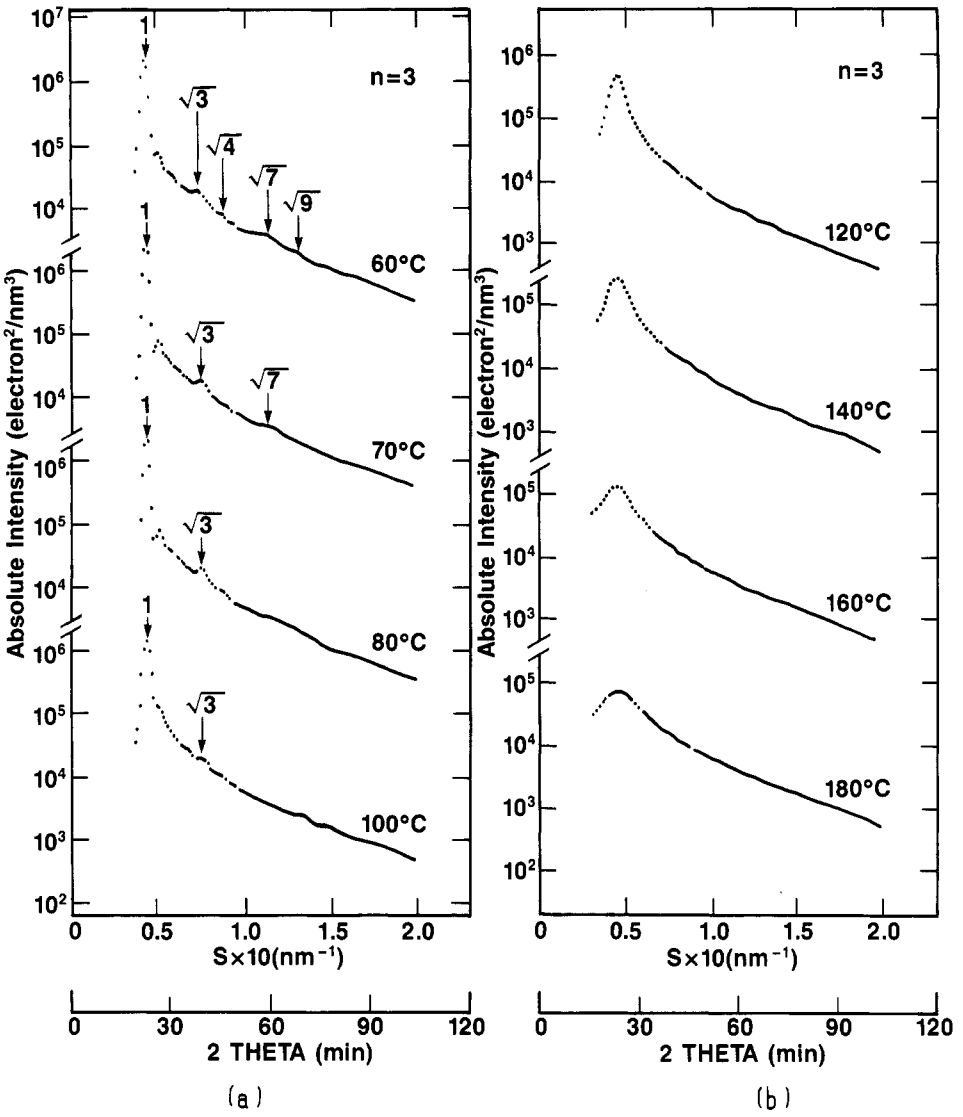


**Figure 1.** Desmeared SAXS profiles for the star block copolymer with $n = 3$ at various temperatures. Absolute SAXS intensities are plotted in logarithmic scale as a function of $2\theta$ or $s = (2 \sin \theta)/\lambda$. $T_b \simeq 110$ °C. $\lambda = 1.54$ Å.

60 to 180 °C where absolute SAXS intensities in logarithmic scale were plotted as a function of $2\theta$ in minutes or $s = (2 \sin \theta)/\lambda = q/2\pi$. This was done in order to present the profiles over a wide range of $2\theta$. The profiles at lower temperatures (part a) show a number of scattering maxima: the higher order maxima exist at the positions of $3^{1/2}$, $4^{1/2}$, $7^{1/2}$, and $9^{1/2}$ relative to the first-order peak,[25] indicating that polystyrene block chains segregate themselves into the cylindrical microdomains in the ordered hexagonal lattice.

As temperature is raised, the higher order peaks gradually disappear, and at $T > 110$ °C (part b of Figure 1) only the first-order maximum can be observed.[32] It will be shown later (section IV, Figure 5) that the order–disorder transition temperature $T_b$ for this copolymer corresponds to 110 °C. In the ordered state (part a of Figure 1) a number of the higher order maxima decrease and the peak position shifts toward larger angles upon elevating temperature, as shown later more clearly in Figures 2 and 3, as a consequence of decreasing segregation power[13] with $T$. On the other hand, in the disordered state (part b of Figure 1), the peak position stays constant but the peak profile broadens upon elevating temperature, as more clearly seen in Figures 2 and 3.

The copolymer with other values of $n$ had the common features to $n = 3$: a long-range order of the microdomains exists in the ordered state at lower temperatures $T \leq T_b$, while at $T > T_b$ the copolymers are in the disordered state, PS and PI blocks being mixed at molecular level.

Figure 2 shows a typical temperature dependence of the first-order SAXS maximum where the absolute intensities were plotted as a function of the scattering angle $2\theta$ in the linear scale for the copolymer with $n = 18$, which has $T_b \simeq 120$ °C, as will be shown in Figure 3. It is clearly seen that in the ordered state (part a of Figure 2) the scattering peak loses its intensity and shifts toward larger angles upon elevating temperature. On the other hand, in the disordered state (part b of Figure 2, $T > T_b \simeq 120$ °C) upon elevating temperature the peak position stays constant but peak intensity decreases, resulting in broader peaks. From the scattering peak position $2\theta_m$, the characteristic size $D$ of the order parameter fluctuation (eq 1) was estimated as a function of temperature, some typical results of which are shown in Figure 3 for $n = 3$, 4, 12, and 18.

As found previously[18] for the copolymers with $n = 1$ and 6 and for the diblock copolymers[13] we can find a crossover in the temperature dependence of $D$ at $T = T_b$ for the all copolymers studied in this work; within experimental accuracy we find the $^1/_3$-power law

$$D_{ord} = f_1(n)T^{-1/3} \tag{15}$$

for ordered state and

$$D_{dis} = f_2(n)T^0 \tag{16}$$

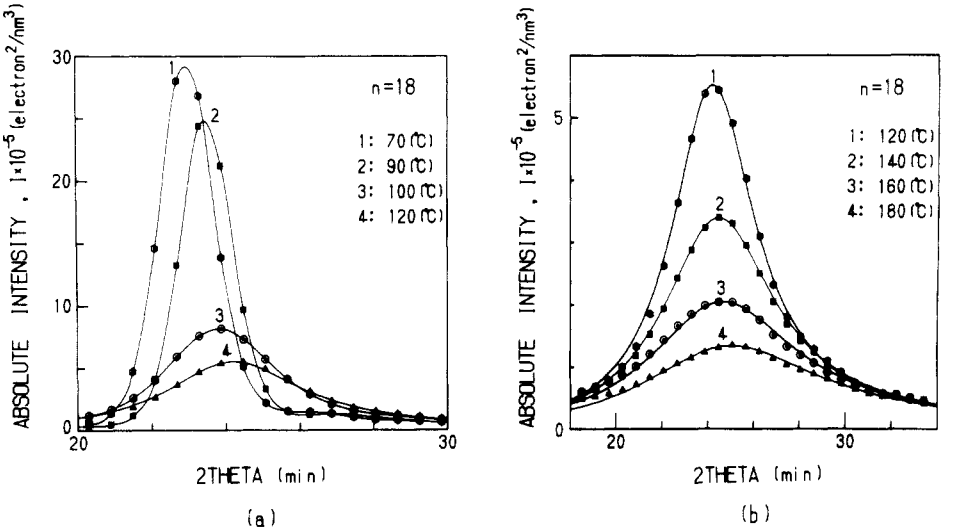


**Figure 2.** Temperature variations of SAXS profiles near the first-order maximum for $n = 18$ where absolute intensities are plotted as a function of $2\theta$ both in linear scales: (a) ordered state and (b) disordered state. $T_b \cong 120$ °C. $\lambda = 1.54$ Å.

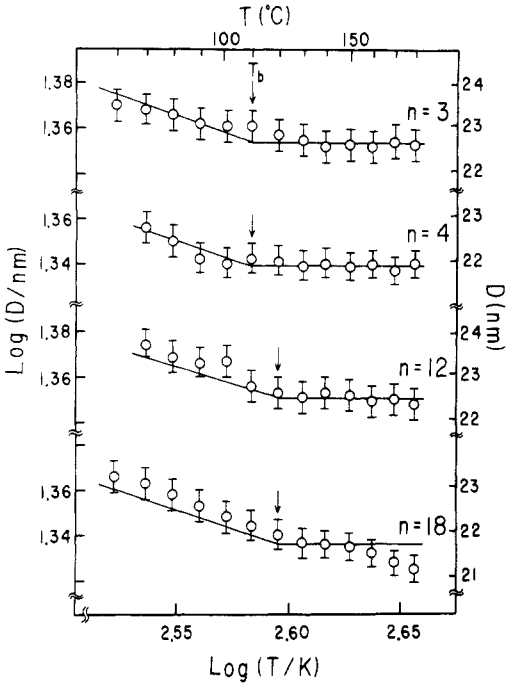


**Figure 3.** Temperature dependence of the characteristic size $D$ of the order parameter in ordered ($T < T_b$) and disordered states ($T \geq T_b$) for some copolymers with $n = 3$, 4, 12, and 18.

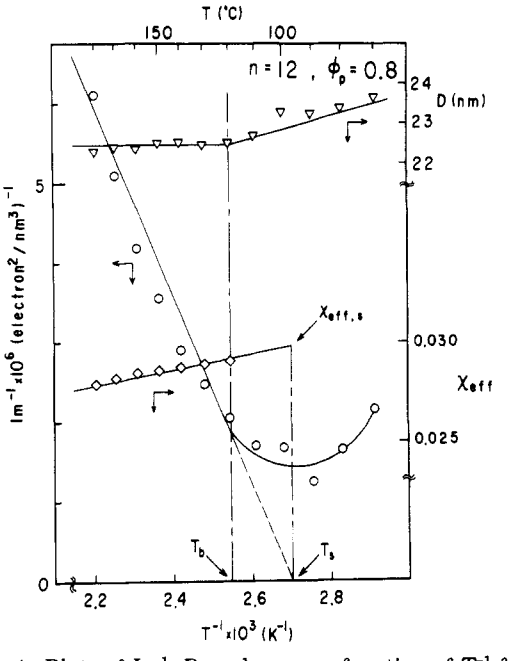


**Figure 4.** Plots of $I_m^{-1}$, $D$, and $\chi_{eff}$ as a function of $T^{-1}$ for the star block copolymer with $n = 12$ and determination of the order–disorder transition temperature $T_b$ from the crossover behavior of $D$ and $I_m^{-1}$ with $T^{-1}$.

for disordered state,[33] where $D_{ord}$ and $D_{dis}$ are the $D$ values for the ordered and disordered states, respectively, and $T$ is absolute temperature.

The spinodal temperature $T_s$ as well as $T_b$ can be determined from temperature dependence of $I_m = I(q = q_{max})$. From eq 3, with increasing $\chi_{eff}$, $I(q)^{-1}$ is expected to decrease linearly for the copolymers in the disordered state, i.e.

$$[I(q)/(a-b)_{eff}^2]^{-1} = S(q)/W(q) - 2\chi_{eff} \quad (17)$$

and reaches to the spinodal point at the wavenumber $q_{max}$

$$I_m^{-1} = I(q_{max})^{-1} \sim S(q_{max})/W(q_{max}) - 2\chi_{eff,s} = 0 \quad (18)$$

where $\chi_{eff,s}$ is the $\chi$-parameter at the spinodal point. If $\chi_{eff}$ has a temperature dependence given by[15,26-28]

$$\chi_{eff} = A' + B'/T \quad (19)$$

then $I_m^{-1}$ is expected to decrease linearly with $T^{-1}$ and goes to zero at $T = T_s$. Figure 4 shows an example of the plot $I_m^{-1}$ vs $T^{-1}$ for $n = 12$ together with the plots of the characteristic size $D$ and $\chi_{eff}$. The method to evaluate $\chi_{eff}$ will be described later (section V-C).

At higher temperatures $T \gtrsim T_b$, $I_m^{-1}$ seems to decrease linearly with $T^{-1}$, although the linearity is observed approximately but not strictly.[29] In this temperature range $D$ is observed to be independent of $T$, as the theory predicts (see eq 3 and discussions in section V-B). Upon further increase of $T^{-1}$, the linearity of $I_m^{-1}$ vs $T^{-1}$ is not observed at all, and this deviation from linearity is accompanied by the deviation of $D$ from the constant value. These two deviations are expected to be a consequence of the order–disorder transition. The temperature $T_b$ was determined from the crossover behaviors of both $D$ and $I_m^{-1}$ with $T^{-1}$ at $T_b$. Furthermore, $T_s$ was determined by extrapolating the linear variation of $I_m^{-1}$ with $T^{-1}$ and by finding $T$ at which $I_m^{-1} = 0$. The temperatures $T_b$ and $T_s$ for all the copolymers were evaluated in this way, and the result is plotted as a function of $n$ in Figure 5.

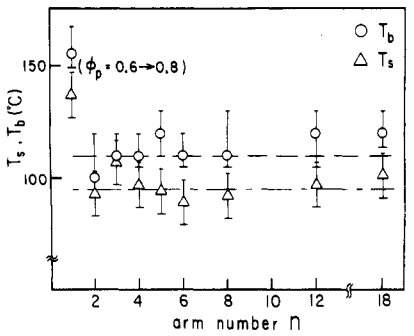


**Figure 5.** Order–disorder transition temperature $T_b$ and the spinodal temperature $T_s$ as a function of $n$.

In Figure 5 a correction was made for the fact that the concentration $\phi_p$ of the copolymer for $n = 1$ ($\phi_p = 0.6$) is lower than those for $n \geq 2$ ($\phi_p = 0.8$). This correction was made by using Flory–Huggins mean-field theory for the neutral solvent[22,23,30]

$$\chi_{eff} = \chi\phi_p \tag{20}$$

where $\chi$ is a bare interaction parameter between the dissimilar monomers in bulk. This equation is expected to be good for such high concentrations[23] as $\phi_p = 0.6$ and 0.8. The data at $\phi_p = 0.6$ for $n = 1$ were converted to those at $\phi_p = 0.8$, by using the formula given below.

$$(A_1 + B_1/T_{s1})\phi_{p1} = (A_1 + B_1/T_{s2})\phi_{p2} \tag{21}$$

$A_1$ and $B_1$, which determine temperature dependence of bare interaction parameter $\chi$ for $n = 1$, are determined by the temperature dependence of $\chi_{eff}$ for $n = 1$. $T_{s1}$ and $T_{s2}$ are the spinodal temperatures for the copolymer with concentrations $\phi_{p1}$ and $\phi_{p2}$, respectively.

The results in Figure 5 indicate that both $T_b$ and $T_s$ drop dramatically by increasing $n$ from 1 to 2 but do not significantly depend on $n$ for $2 \leq n \leq 18$. This is one of the most important experimental results found in this study.

## V. Interpretations

**A. Fluctuations in Ordered State.** The characteristic size $D$ of the order parameter fluctuation in the ordered state ($D_{ord}$) is observed as a function of $n$ and $T$, the results of which were partially shown in Figure 3 and in eq 15. Here we discuss $D_{ord}$ as a function of $n$ and $T$.

The continuity of $D$ in the ordered and disordered states at $T = T_b$ invokes that

$$D_{ord}(n,T) = D_{dis}(n)(T/T_b)^{-1/3} \quad \text{for} \quad T/T_b \leq 1 \tag{22}$$

if the temperature exponents, $-1/3$ and 0, are independent of $n$ for the ordered and disordered state, respectively.

Figure 6 shows an experimental test of the scaling behavior of eq 22 where log ($D_{ord}/D_{dis}$) are plotted against log ($T/T_b$) for the all copolymers listed in Table I. The result assures the scaling behavior within experimental accuracy. Then $D_{ord}(n,T)$ will be predicted from $D_{dis}(n)$ for the disordered state and the order–disorder transition temperature $T_b$.

**B. Fluctuation Spectrum in Disordered State.** Here, we extensively discuss the spectrum of the order parameter fluctuations in the disordered state. Figure 7 shows SAXS profiles in the disordered state at various $T(>T_b)$ for some copolymers with $n = 2$, 4, 12, and 18. The measured SAXS profiles shown by data points were best fitted with the theoretical profiles obtained from eq 3 and drawn by solid lines. Good agreement between theoretical and experimental profiles is found for other copolymers also. The best fits yield information on $R_g^2 = N_0a^2/6$ for the arm block copolymer and on $\chi_{eff}$ as a function of $T$ and

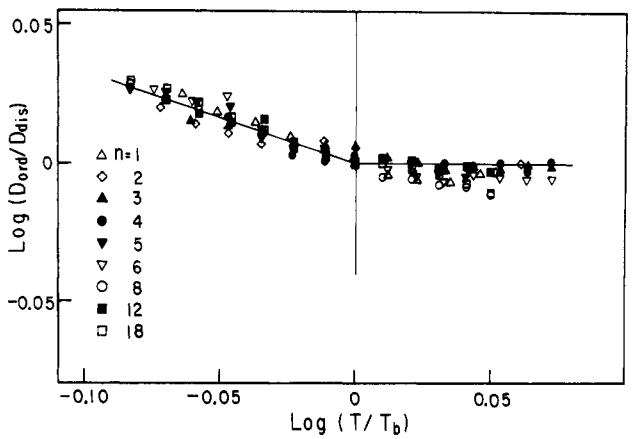


**Figure 6.** Master curve for the reduced characteristic size of the order parameter $D_{ord}/D_{dis}$ as a function of the reduced temperature $T/T_b$, where $D_{ord}$ and $D_{dis}$ are the sizes in the ordered and disordered states, respectively, and $T_b$ is the order–disorder transition temperature.

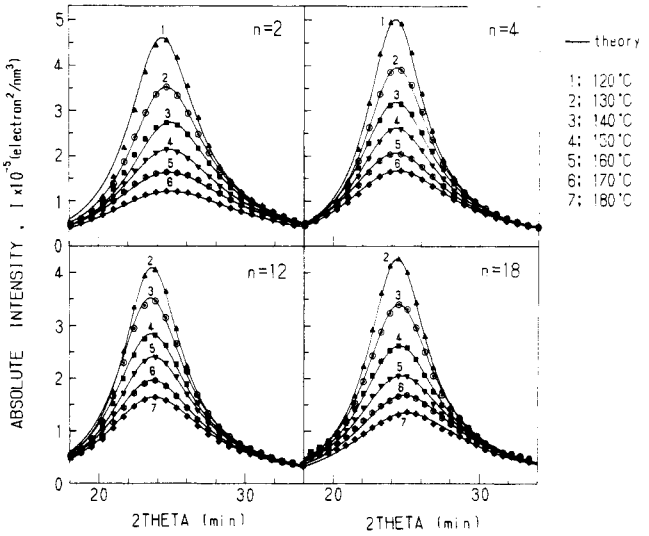


**Figure 7.** Typical SAXS profiles of the star block copolymes in the disordered state. Experimental and theoretical profiles are shown, respectively, by data points and solid lines. $\lambda = 1.54$ Å.

$n$, which will be discussed in sections V-E and V-C, respectively.

Experimental results indicate that the wavenumber $q_{max}$ for the dominant mode of the fluctuations for a given copolymer is independent of $T$[33] as theory predicts and that $q_{max}$ depends on $n$. The $n$-dependence of $q_{max}$ and a comparison of it with the theoretical result will be referred to in section V-E.

The fluctuation spectrum in the limit of $\chi = 0$, i.e., the spectrum purely related to molecular conformation of the copolymer as given by $W(q)/S(q)$ (eq 17), can be analyzed experimentally as shown in Figure 8 for $n = 6$, as an example, where $[I(q)/C]^{-1}$ were plotted as a function of $q$ at various temperatures $T$ ($\geq T_b$). $C$ is a constant equal to $(a - b)_{eff}^2 = (a - b)^2\phi_p$. From eq 17 all the profiles at different temperatures (as shown in the left-hand side of Figure 8) should have the same $q$-dependence if the conformation is essentially unaltered at $T \geq T_b$, which is will expected to be valid over a narrow temperature range covered in this experiment, and should be superimposable along a vertical shift by the amount of $2\chi_{eff}(T)$. In fact as shown in the right-hand side of Figure 8, these curves are found to be satisfactorily superimposed to each other by the vertical shift to result in a master curve, i.e., S-

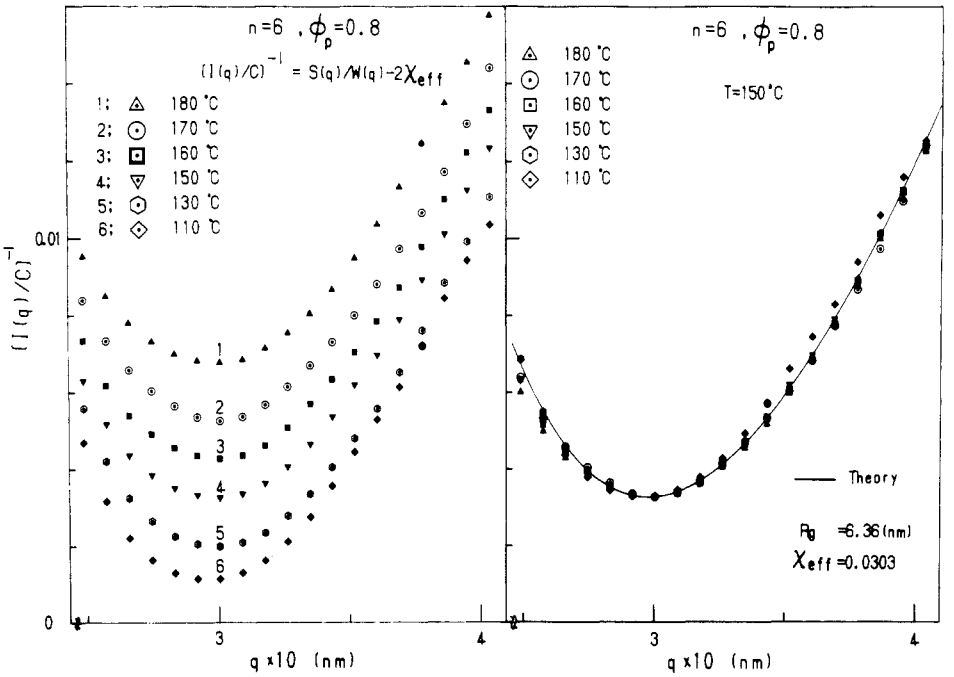


**Figure 8.** Experimental profiles for $[S(q)/W(q) - 2\chi_{eff}]$ for the star block copolymer with $n = 6$ at various temperatures (left-hand side), and the maste curve obtained at $T = 150$ °C by the vertical shifts of the profiles at various temperatures (right-hand side).

$(q)/W(q) - 2\chi_{eff}$ at 150 °C. Thus, $S(q)/W(q)$ can be obtained by shifting the master curve vertically by an amount of $2\chi_{eff} = 0.0606$.

The relative $q$-dependence of $S(q)/W(q)$ shown by the master curve can be compared to the profile predicted by the RPA theory (eq 3-14). The theoretical profile drawn by a solid line is found to be in good agreement with the experimental profile. The best fit is obtained for $R_g = (N_0a^2/6)^{1/2} = 6.36$ nm.

The master curves for $S(q)/W(q)$ for other copolymers also are obtained, and they show a reduction at a level similar to the reduction for $n = 6$. They are found to agree with the corresponding theoretical profile with an accuracy similar to that for $n = 6$.

**C. Determination of $\chi$-Parameters.** The effective thermodynamic interaction parameters, $\chi_{eff}$, are obtained as a function of $n$ and $T$ by best fitting the theoretical and experimental profiles in the disordered state as shown in Figure 7. Temperature dependencies of $\chi_{eff}$ thus estimated are shown in Figure 9 for all the copolymers studied here. Figure 9 includes also $T_b$ or $\chi_{eff}(T_b)$ shown by arrows and $T_s$ or $\chi_{eff,s}$ by solid circles.

It is important to note that $\chi_{eff}$ is not independent of $n$ but rather has a *remarkable n-dependence*, the greater the value $n$, the smaller is the value $\chi_{eff}$. The result clearly indicates that the theory has to be generalized in order to account for effects of the connectivity of the arm blocks at the center of the star block copolymer on the local conformation of the arms, segmental packing, and hence the segmental interactions. It is also interesting to note that a drastic change on the $\chi_{eff}$ with $n$ occurs between $n = 1$ and 2.[31]

Temperature dependence of $\chi_{eff}$ shows approximately $1/T$ dependence as given by eq 19, although it shows a weak but systematic deviation from $1/T$ dependence. All the curves for $\chi_{eff}$ $(1/T)$ show slightly convex nature, i.e., a downward deviation from the linearity at small $1/T$. This deviation becomes less remarkable as the level of $\chi_{eff}$ decreases. The entropic and enthalpic part of the $\chi_{eff}$ (i.e. $A'$ and $B'$ in eq 19, respectively) are plotted as a function of $n$ in Figure 10. Here again the data for $n = 1$, which were obtained for $\phi_p = 0.6$ were converted to those for $\phi_p$

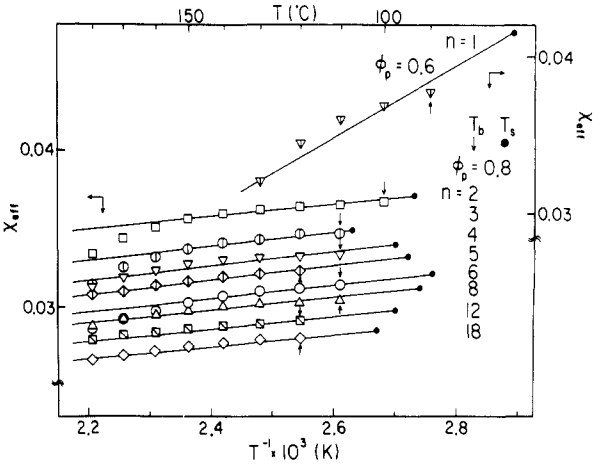


**Figure 9.** Temperature dependence of the estimated $\chi_{eff}$ for the star block copolymers studied in this work. The arrows indicate the order–disorder transition temperature $T_b$ and $\chi_{eff,b} = \chi_{eff}$ $(T = T_b)$, and the solid circles indicate the spinodal temperature $T_s$ and $\chi_{eff,s}$.

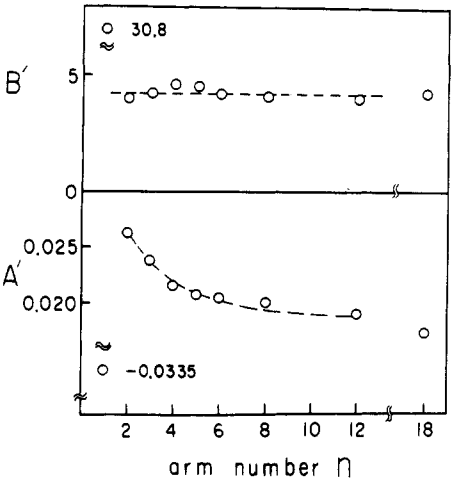


**Figure 10.** Temperature dependence of $A'$ and $B'$ when $\chi_{eff}(T)$ is assumed to be given by $\chi_{eff}(T) = A' + B'/T$ for all the star block copolymers studied in this work.

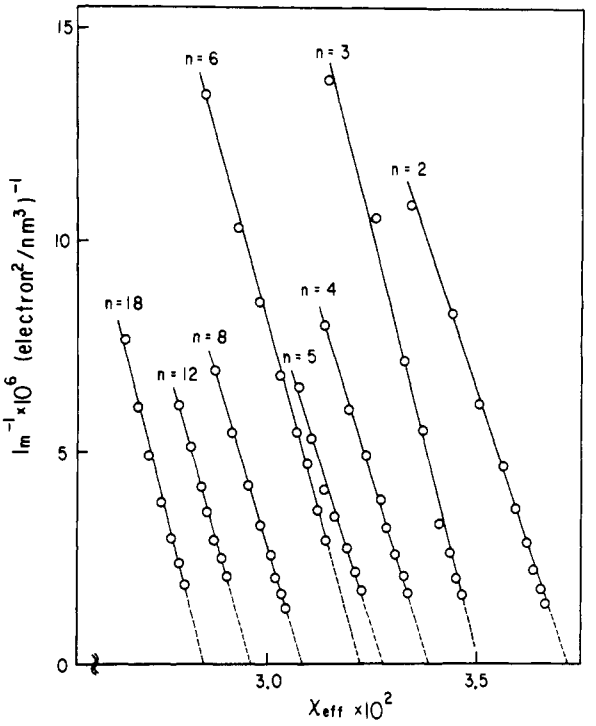


**Figure 11.** $I_m^{-1}$ as a function of $\chi_{eff}$ assuring eq 17. The intercepts with abscissa give $\chi_{eff,s}$ as a function of $n$.

= 0.8 by using the scheme as discussed earlier in connection with Figure 5 and eq 20 and 21. Again, a big jump in the values $A'$ and $B'$ are observed by increasing $n$ from $n = 1$ to 2. It is also interesting to note that $B'$ stays constant but $A'$ decreases with $n$ for $n \geq 2$, which clearly reflects an effect of the connectivity of the arms at its center.

It should be noted that the slight deviation in the $\chi_{eff}(T)$ from the $1/T$-dependence causes also the deviation of the $I_m^{-1}(T)$ from the $1/T$-dependence at $T \geq T_b$ as discussed earlier in section IV[29] in connection with Figure 4. It should be noted also that $\chi_{eff}$ in Figure 4 was determined by the procedure as discussed in this section. Instead of plotting $I_m^{-1}$ with $T^{-1}$, one can plot $I_m^{-1}$ with $\chi_{eff}$, since $\chi_{eff}(T)$ is known. Then we should be able to obtain linear dependencies of $I_m^{-1}$ with $\chi_{eff}$ at $T \geq T_b$. In fact we could obtain good linear dependencies for all the copolymer as shown in Figure 11 at $T \geq T_b$ (solid lines), in agreement with prediction by eq 17. At $T < T_b$ (or $\chi_{eff} > \chi_{eff,b} = \chi_{eff}(T_b)$), the deviation of $I_m^{-1}$ vs $\chi_{eff}$ from the straight line occurs, which is obviously due to the onset of order formation (disorder-to-order transition). Hence, a straight line above $T \geq T_b$ was extrapolated down to $I_m^{-1} = 0$ to obtain the mean-field spinodal point, $\chi_{eff,s}$. The extrapolated portions, which correspond to the ordered state, are shown by broken lines.

**D. Stability Limit and Order–Disorder Transition.** The stability limit ($T_s$ and $\chi_{eff,s}$) and order–disorder transition ($T_b$ and $\chi_{eff,b} = \chi_{eff}(T_b)$) were obtained as a function of $n$ by the method discussed in section IV in connection with Figure 4. The values $\chi_{eff,s}$ are also obtained from the plots shown in Figure 11 by extrapolating $I_m^{-1}$ to zero and finding the intercepts with the abscissa. The $\chi_{eff}$'s obtained by these two methods should agree with each other and in fact agreed within experimental accuracy.

The $\chi$-parameters at the spinodal points ($\chi_{eff,s}$) and at the order–disorder transition points ($\chi_{eff,b}$) are plotted as a function of $n$ and compared with the theoretical spinodal point $(1/2)S(q_{max})/W(q_{max}) = \chi_s$ in Figure 12. As seen

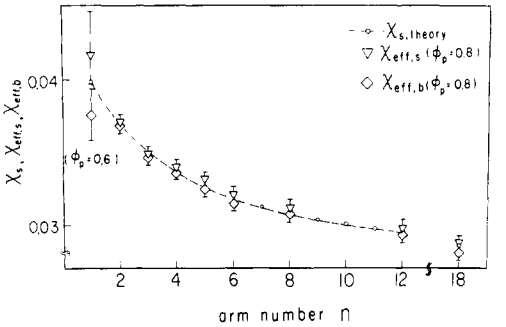


**Figure 12.** $\chi_{eff}$ at the spinodal point ($\chi_{eff,s}$) and at the order–disorder transition ($\chi_{eff,b}$) as a function of $n$ and comparisons of them with the theoretical value $\chi_s$ at the spinodal points, $\chi_s = (1/2)S(q_{max})/W(q_{max})$.

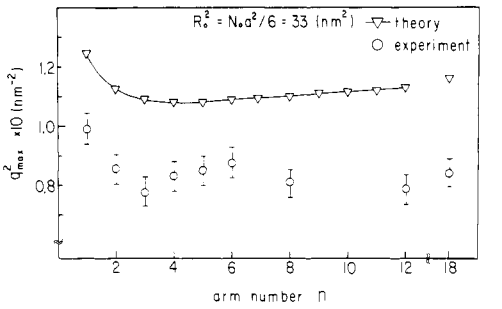


**Figure 13.** Experimental and theoretical values of $q_{max}^2$ as a function of $n$. The theoretical values are obtained by setting the mean-squared unperturbed radius of gyration $R_0^2 = N_0a^2/6 = 33$ nm$^2$.

in Figure 12, $\chi_{eff,s}$ is slightly but significantly larger than $\chi_{eff,b}$. This trend is also clearly seen in Figure 5. The theoretical values $\chi_s$ agree quite well with the experimental values $\chi_{eff,s}$, both of which decrease with increasing $n$. However, it should be noted that the decrease of $\chi_s$ with $n$ does not necessarily imply the increase of $T_s$ with $n$ in the case when $\chi$ depends on $n$. In fact the decrease of $\chi_{eff,s}$ or $\chi_s$ with $n$ is compensated by the decrease of $\chi_{eff}$ with $n$, giving rise to $T_s$ nearly independent of $n$, as shown in Figure 5 for $n > 2$.

**E. Wavenumber $q_{max}$ of Dominant Mode of Fluctuations.** Figure 13 compares experimental and theoretical values of the wavenumber in the dominant mode of the fluctuations for the series of the star block copolymers. The theoretical values $q_{max}^2$ as a function of $n$ are obtained by using $R_g^2 = N_0a^2/6 = 33$ nm$^2$ for the arm block chain, which is estimated on the basis of the reported unperturbed dimensions for both PS and PI.[18] As found previously for $n = 1$ and 6 we find again a discrepancy of $q_{max,theor}/q_{max,exp} \simeq 1.1$ or $D_{dis,exp}/D_{dis,theor} \simeq 1.1$ for all $n$ where $q_{max,theor}$ and $q_{max,exp}$ are the theoretical and experimental values of $q_{max}$, respectively, and $D_{dis,theor}$ and $D_{dis,exp}$ are those for $D_{dis}$. The discrepancy may be due to the effects of polydispersities of molecular weight and those of composition of the arm as pointed out in the previous paper[18] or the effects of asymmetry among the ams caused again by the polydispersities of the molecule weight and composition. The deviation may be due also to chain expansion existing even in concentrated solutions.[34]

**Acknowledgment.** We are grateful to M. Olvera de la Cruz, I. Sanchez, E. L. Thomas, H. Hasegawa, and H. Tanaka for useful discussions and comments. The Kyoto University group thanks the Ministry of Education, Science and Cultue, Japan, for a partial financial support of this work by a Grant-in-Aid for Scientific Research (63470090).

**Registry No.** (Styrene)(isoprene) (block copolymer), 105729-79-1.

## References and Notes


(1) de Gennes, P. G. *Scaling Concept in Polymer Physics*; Cornell University: Ithaca, NY, 1979.
(2) LeGrand, A. D.; LeGrand, D. G. *Macromolecules* **1979**, *12*, 450.
(3) Leibler, L. *Macromolecules* **1980**, *13*, 1602.
(4) Leibler, L.; Benoit, H. *Polymer* **1981**, *22*, 195.
(5) Benmouna, M.; Benoit, H. *J. Polym. Sci., Polym. Phys. Ed.* **1983**, *21*, 1227.
(6) Olvera de la Cruz, M.; Sanchez, I. *Macromolecules* **1986**, *19*, 2501.
(7) Mori, K.; Tanaka, H.; Hashimoto, T. *Macromolecules* **1987**, *20*, 381.
(8) Benoit, H.; Hadziioannou, G. *Macromolecules* **1988**, *21*, 1449.
(9) Ijichi, Y.; Hashimoto, T. *Polym. Commun.* **1988**, *29*, 135.
(10) Tanaka, H.; Hashimoto, T. *Polym. Commun.* **1988**, *29*, 212.
(11) See, for example: Hashimoto, T. In *Thermoplastic Elastomers*; Legge, N. R., Holden, G., Schroeder, H. E., Eds.; Hanser: Vienna, 1987; Chapter 12.3.
(12) Roe, R. J.; Fishkis, M.; Chang, C. J. *Macromolecules* **1981**, *14*, 1091.
(13) Hashimoto, T.; Shibayama, M.; Kawai, H. *Polym. Prepr. (Am. Chem. Soc., Div. Polym. Chem.)* **1982**, *23*, 21; *Macromolecules* **1983**, *16*, 1093.
(14) Hashimoto, T.; Tsukahara, Y.; Kawai, H. *Polym. J. (Tokyo)* **1983**, *15*, 699.
(15) Mori, K.; Hasegawa, H.; Hashimoto, T. *Polym. J.* **1985**, *17*, 799.
(16) Bates, F. S.; Hartney, M. A. *Macromolecules* **1985**, *18*, 2478. Bates, F. S. *Macromolecules* **1987**, *20*, 2221.
(17) Nojima, S.; Roe, R. J. *Macromolecules* **1987**, *20*, 1866.
(18) Hashimoto, T.; Ijichi, Y.; Fetters, L. J. *J. Chem. Phys.* **1988**, *89*, 2463.
(19) Fredrickson, G. H.; Helfand, E. *J. Chem. Phys.* **1987**, *87*, 697.
(20) Fetters, L. J.; Richards, R. W.; Thomas, E. L. *Polymer* **1987**, *20*, 2252.
(21) Thomas, E. L.; Alward, D. B.; Kinning, D. J.; Martin, D. C.; Handlin, D. L.; Fetters, L. J. *Macromolecules* **1986**, *19*, 2197.
(22) Hashimoto, T.; Sasaki, K.; Kawai, H. *Macromolecules* **1984**, *17*, 2812. Sasaki, K.; Hashimoto, T. *Macromolecules* **1984**, *17*, 2818.
(23) Onuki, A.; Hashimoto, T. *Macromolecules*, in press.
(24) The SAXS profiles were obtained for Cu K$\alpha$ radiation ($\lambda$ = 1.54 Å).
(25) The scattering maximum that exists at $2\theta$, only slightly higher than the first-order maximum, is an artifact caused by instability of the desmearing procedure of the very sharp first-order peak.
(26) Rounds, N. A., and McIntyre, D., cited in: Helfand, E.; Wasserman, Z. R. *Macromolecules* **1976**, *9*, 879.
(27) Roe, R. J.; Zin, C. W. *Macromolecules* **1980**, *13*, 1221.
(28) Shibayama, M.; Yang, S. H.; Stein, R. S.; Han, C. C. *Macromolecules* **1985**, *18*, 2179.
(29) A weak curvature is seen at $T > T_b$, but this curvature is small compared with the curvature existing at $T \geq T_b$. The latter large curvature bears a more physical significance and indicates the onset of order formation (order–disorder transition). The weak curvature at $T > T_b$ may be due to a consequence of a slight deviation of $\chi_{eff}(T)$ from the $1/T$ dependence as seen in Figure 4 (of a slightly convex nature). This idea is supported, because $I_m^{-1}$ linearly decreases with $\chi_{eff}$ at $T > T_b$ as seen in Figure 11, where $I_m^{-1}$ is plotted against $\chi_{eff}$ itself rather than $1/T$. The weak curvature may arise also from the nonclassical effect.[19]
(30) Helfand, E.; Tagami, Y. *J. Chem. Phys.* **1972**, *56*, 3592.
(31) This may be due to the corrections to the mean field value of $\chi_{eff} = \chi\phi_p$. The detailed analyses on the corrections will be deferred until we get precise values for $\chi_{1s}$ and $\chi_{2s}$, the $\chi$-parameters between the polymers and solvent. However, if $\chi_{1s} \simeq \chi_{2s} \simeq 0.45$, as in the case of polystyrene/polyisoprene/toluene, $\phi_p = 0.6$–$0.8 \gg f_0 = (1 - 2\chi_{1s})/u^* \simeq 0.02$, so that the block copolymer solutions are in $\theta$ state. Further $\phi_p \gg \chi_{12}/u_{12}^* = 0.01$–$0.5$, so that the renormalization group effect is expected to be small (see ref 23 for details). In this case we expect the mean field value of $\chi_{eff} = \chi\phi_p$ is correct.
(32) Subsidiary maxima that are weak but occasionally seen in the profiles at $T \geq 120$ °C (part b, Figure 1) are not reproducible and should be regarded as artifacts. However, the maxima in the profiles at lower temperatures, $T \leq 100$ °C (part a, Figure 1), marked by arrows are reproducible.
(33) Close observation of the results in Figures 3 and 6, some data especially those for $n = 8$ and 18, tend to show a tendency of decreasing $D_{dis}$ with increasing $T$. However, it is difficult to claim positively that $D_{dis}$ decreases with $T$ within experimental accuracy. Within experimental accuracy and judging from the data for all $n$, it is fair to say that $D_{dis}$ is independent of $T$. There appear to be more important discussions here. That is, as we pointed out previously,[18] it is difficult to decide unequivocally at present whether the transition between the ordered state ($D_{ord}$ being temperature dependent) and the disordered state ($D_{dis}$ being temperature independent) is sharp or gradual. Here we take a simplified picture, i.e., the sharp transition as a starting step.
(34) In fact, the chain expansion near the core of star block or star branched polymers was observed in dilute solution and the melt.[35] This expansion may also cause the expansion of the arm chain as a whole.
(35) Lantman, C. W.; MacKnight, W. J.; Rennie, A. R.; Tassin, J. F.; Monnerie, L.; Fetters, L. J. *Macromolecules*, in press. Horton, J. C.; Squires, G. L.; Boothroyd, A. T.; Fetters, L. J.; Rennie, A. R.; Glinka, C. J.; Robinson, R. A. *Macromolecules* **1989**, *22*, 681. Boothroyd, A. T.; Squires, G. L.; Fetters, L. J.; Rennie, A. R.; Horton, J. C.; de Vallêra, A. M. B. G. *Macromolecules*, in press.


# Studies on Copolymeric Hydrogels of *N*-Vinyl-2-pyrrolidone with 2-Hydroxyethyl Methacrylate

**Thomas P. Davis† and Malcolm B. Huglin***

*Department of Chemistry and Applied Chemistry, University of Salford, Salford M5 4WT, England.* *Received February 20, 1988; Revised Manuscript Received November 15, 1988*

ABSTRACT: *N*-Vinyl-2-pyrrolidone and 2-hydroxyethyl methacrylate in both the absence and the presence of ethylene glycol dimethacrylate have been copolymerized to high conversion by $\gamma$-irradiation. The resultant xerogels were swollen to equilibrium in water to yield hydrogels. The effects of monomer composition and concentration of added cross-linking agent on the swelling behavior and mechanical properties of these hydrogels at 294 K were investigated, the latter involving measurements of stress (compression)–strain. The findings were interpreted on the basis of terpolymer compositional drift as predicted by the *Q*–*e* scheme. Inhomogeneous cross-linking of the copolymer network was noted particularly at high contents of *N*-vinyl-2-pyrrolidone.

## Introduction

The following abbreviations are adopted in the text: BA, *n*-butyl acrylate; EDMA, ethylene glycol dimethacrylate; EWC, equilibrium water content (=wt % water in hydrogel at equilibrium); HEMA, 2-hydroxyethyl methacrylate; VP, *N*-vinyl-2-pyrrolidone; TPT, 1,1,1-trimethylolpropane trimethacrylate. In addition, the polymeric form is prefixed where appropriate by P-.

In the authors' laboratory recent studies have been devoted to uniaxial compression and swelling measurements

† Present address: Institute for Polymer Research, Department of Chemical Engineering, University of Waterloo, Waterloo, Ontario N2L 3G1, Canada.

0024-9297/89/2222-2824$01.50/0 